Dynamic Node Lifetime Estimation (DNLE) for Wireless Sensor Networks

Wilawan Rukpakavong, Lin Guan, and Iain Phillips

***Abstract*—Wireless Sensor Networks (WSNs) consist of a large number of nodes each with limited battery power. As networks of these nodes are usually deployed unattended, network lifetime becomes an important concern. This paper proposes a novel, feasible, dynamic approach for node lifetime estimation that works for both static and dynamic loads. It covers several factors that have an impact on node lifetime, including battery type, model, brand, self-discharge, discharge rate, age and temperature. The feasibility of the proposed scheme is evaluated by using the real testbed experiments with two wireless sensor platforms: Mica2 and N740 NanoSensor, two operating systems: TinyOS and Contiki, and different brands of alkaline and Nickel-Metal-Hydride (NiMH) batteries. The deviation of the proposed estimation is in the range of $-3.5\,\%$ to $2.5\,\%$. Three major contributions are presented in this paper: (1) the impact factors on node lifetime; (2) lifetime equations for any starting voltage, ageing, charge cycles and temperatures; (3) the dynamic node lifetime estimation technique (DNLE), which is proposed and implemented on real hardware and software platforms in WSNs.**

***Index Terms*—Lifetime, battery capacity, current consumption, wireless sensor networks.**

I. Introduction

WIRELESS sensor networks (WSNs) have two critical constraints: the first is that sensor nodes are often battery powered and thus have limited energy budgets; the second is that sensor nodes have a large number of nodes and usually deployed unattended, causing difficulty when replacing or recharging batteries across the entire network. Therefore, network lifetime (i.e. time while the network is usefully working) is an important issue. With accurate lifetime estimation of the sensor nodes, application designers can prevent service interruptions for critical applications. Moreover, many protocol layers, such as the MAC and routing layers, are able to make intelligent decisions that can help conserve energy and prolong lifetime.

Two important factors: battery capacity and current consumption are used for node lifetime estimation. In many studies [1]–[4], quoted capacity and calculations based on data sheets are usually used for battery capacity and measurements made for current consumption estimation. Furthermore, a fixed temperature is normally assumed (e.g., $25\,^{\circ}$C). This means that running a static load program multiple times always consumes the same energy. However, in reality, programs will have different energy requirements resulting in different lifetimes [5]. Furthermore, the non-linear behaviour of the batteries needs to be taken into account. The challenge is to find an accurate lifetime estimation technique that covers temperature, battery age and self-discharge as well as other impact factors on node lifetime.

This paper proposes Dynamic Node Lifetime Estimation (DNLE), an approach that includes an investigation of the impact factors on node lifetime. DNLE has been implemented on real hardware: Mica2 [6] and N740 NanoSensor [7], and software platforms: TinyOS [8] and Contiki [9], [10]. Two common types of AA-size batteries: alkaline and NiMH have been investigated. This paper is organised as follows. Section II discusses the existing lifetime estimation algorithms. The impact factors on lifetime are examined in Section III. Section IV explains the design and implementation of the proposed method: DNLE. In Section V, an evaluation of DNLE is presented. Finally, Section VI is the conclusions and future work.

Manuscript received September 23, 2013; revised November 07, 2013; accepted December 1, 2013; Date of publiction mmmm dd, 2014; date of current version mmmm dd, 2014. The associate editor coordinating the review of this paper and approving it for publication was Prof. Kiseon Kim.

W. Rukpapavong, L. Guan and I. Phillips are with the Department of Computer Science, Loughborough University, Leics, LE11 3TU, UK. e-mail: (W.Rukpakavong@lboro.ac.uk; L.Guan@lboro.ac.uk; I.W.Phillips@lboro.ac.uk).

II. Existing Lifetime Estimation Models

The lifetime (Lt) of a sensor node can be considered to depend on two factors, the capacity of the battery (C) and current consumption needed by that node (I), which is expressed as [11]:

$$Lt = \frac{C}{I^k} \tag{1}$$

where k is the peukert constant, which depends on battery type [11]–[14]. It is therefore necessary to estimate both battery capacity and current consumption as well as have a knowledge of the battery type to determine an estimate of node lifetime.

A. Battery Capacity Estimation

There are several methods for determining the State of Charge (SoC) of the battery. This paper focuses the methods of electrochemical, voltage measurement, load testing and the electromotive force, which can be applied for alkaline and NiMH battery capacity estimation.

1) Electrochemical method: Since chemical energy in battery cells is converted into electrical energy through an electrochemical reaction, many studies [15], [16] propose electrochemical models based on the chemical processes that take place in the battery. These models describe the battery processes in great detail. However, they are very complex

and require highly detailed knowledge of the electrochemical process, which makes them difficult to configure and deploy. An easy and accurate way is provided by measuring the specific gravity of the electrolyte in the battery using a hydrometer [11]. The specific gravity varies according to SoC level. When the SoC level decreases, the density of the electrolyte becomes lighter and the specific gravity becomes lower. An example of the relationship between the specific gravity and SoC is shown in Table I [11].

TABLE I
THE RELATIONSHIP BETWEEN THE SPECIFIC GRAVITY AND SOC [11]

Specific Gravity	SoC (%)
1.265	100
1.239	75
1.200	50
1.170	25
<1.110	0

2) Voltage Measurement: Voltage measurement is a popular method for estimating current capacity, especially for mobile phone applications. For example, Heyer [17], [18] introduced a single-meter device for indicating the battery capacity on the basis of the measured battery voltage. This technique requires a look-up table in which fixed voltage values are stored and used in order to indicate SoC. For example, table II provides the relationship between voltage and SoC for Energizer NiMH battery [13].

TABLE II
THE RELATIONSHIP BETWEEN OUTPUT VOLTAGE AND SOC [13]

Voltage (V)	SoC (%)
1.45	100
1.34	90
1.30	80
1.28	50-70
1.27	40
1.25	30
1.22	20
1.14	10
<1	0

3) The ElectroMotive Force (EMF): The EMF is the internal driving force of a battery, providing energy to a load. Many studies [11], [19] found that there is a good linear relationship between the EMF and the SoC and this relationship does not change during cycling of the battery. To estimate SoC based on the EMF, a piecewise linear function is required. The intervals in voltage and the corresponding SoC are presented in Table III [11]:

$$SoC = SoC_{low} + \frac{V_m - V_{low}}{V_{high} - V_{low}} \left(SoC_{high} - SoC_{low}\right) \quad (2)$$

where V_m is the measured battery voltage value, V_{low} and V_{high} are the specific values from the EMF curve for the voltages corresponding to the SoC_{low} and SoC_{high}, e.g., in Table III, V_{low} = 4.08 and V_{high} = 4.24 corresponding to SoC_{low} = 85 and SoC_{high} = 100, respectively. Therefore, the capacity of battery at $4.10\,\mathrm{V}$ is $\approx 87\,\%$ of maximum.

TABLE III
THE INTERVALS IN VOLTAGE AND THE CORRESPONDING SOC FOR SONY US18500G3 LI-ION BATTERY [11]

Interval number	Interval Voltage(V)	SoC(%)
1	4.08-4.24	85.0-100
2	4.06-4.08	81.7-85.0
3	4.02-4.06	76.7-81.7
4	3.98-4.02	73.4-76.7
5	3.88-3.98	58.4-73.4
6	3.80-3.88	22.0-58.4
7	3.68-3.80	8.7-22.0
8	3.54-3.68	5.4-8.7
9	3.32-3.54	2.1-5.4
10	3.00-3.32	0.5-2.1
11	2.50-3.00	0.0-0.5

4) Load Testing: Battery capacity drops due to many factors, such as ageing and life cycle. Battery capacity testing by a load tester serves to determine the actual capacity of the battery. The load is usually designed to represent the expected conditions in which the battery may be used. With a battery load tester, a specific discharge current is applied to the battery while measuring the voltage drop. This is the most accurate and reliable battery testing technique [17]. Many battery load tester products support both alkaline and NiMH batteries, such as the ZTS MBT-MIL Multi-Battery Tester [20] and Ansmann Energy Check LCD Battery Tester [21]. However, these products automatically initiate a timed pulse load test on the battery upon detection in a terminal. This load test cannot be modified. In addition, these testers do not provide information related to temperature. The Computerised Battery Analyser-III (CBA-III) [22], a product from the West Mountain Radio, is a computer calibrated for high accuracy which uses an on-board microcontroller. A pulse width modulation system is used for controlling a pair of power MOS FET transistors using both electronic and software current regulation. The CBA-III allows for defining the load test from $0.1\,\mathrm{A}$ to $40\,\mathrm{A}$. Moreover, it provides information about the total amount of energy stored in a battery (capacity in amp-hours) and graphically displays and charts voltage versus amp-hours. Furthermore, a CBA-III supports the temperature measurement of a battery under test using the external temperature probe. In addition, a computer can connect to CBA-III via the USB interface on-board microcontroller for collecting the data.

5) Temperature Effect: Based on the famous Arrhenius equation, Sheridan et al. [23] proposed the ratio of capacity at two different temperatures in Kelvin (T_1, T_2) as:

$$\frac{C(T_2)}{C(T_1)} = \exp\left(A \cdot \frac{(T_2 - T_1)}{T_2 \cdot T_1}\right) \quad (3)$$

where A is a constant value obtained by dividing the activation energy (in $\mathrm{J\,mol^{-1}}$) with the gas constant (in $\mathrm{J\,mol^{-1}\,K^{-1}}$) of the battery. The relationship between battery capacity and lifetime was studied experimentally by Nguyen et al. [2] for different alkaline battery brands. The effect of temperature on NiMH battery capacity with different commercial AA-size NiMH batteries was explored by Pierozynski [24]. His work reported that the battery capacity is almost equal $96\,\%$ at room temperature and it is dropped to $74\,\%$ at $-20\,^{\circ}\mathrm{C}$ and $58\,\%$ at

$-30\,^{\circ}\mathrm{C}$. The model proposed by Park et al. [25] covered the remaining capacity and the effect of temperature on battery capacity. From their experiment with rising temperature of $20\,^{\circ}\mathrm{C}$ to $60\,^{\circ}\mathrm{C}$, it was observed that the battery capacity increases around $0.5\,\%$ of SoC when temperature increases by $1\,^{\circ}\mathrm{C}$. With decreasing temperature from $20\,^{\circ}\mathrm{C}$ to $-10\,^{\circ}\mathrm{C}$, the battery capacity decreases $1.7\,\%$ of SoC when temperature decreases $1\,^{\circ}\mathrm{C}$.

B. Current Consumption Estimation

There are several methods for determining the current consumption of sensor nodes. The existing mechanisms are hardware-based, software-based and include temperature effect supply voltage changes.

1) Hardware-based Mechanism: To estimate node current consumption, many current consumption models [26], [27] tried to design the special circuits for finding the average leakage current consumption; however, detailed knowledge of electrical circuits is required. Oscilloscopes or ammeters are commercially available for measuring the current draw from the circuit of sensor nodes with accurate results. Since the unique characteristics of sensor network applications make it difficult to measure the power and current consumption of each sensor node, Jiang et al. [28] developed hardware-based integrated circuits attached to sensor node boards for measuring the current consumption. This mechanism can capture phenomena such as per-node fluctuations.

2) Software-based Mechanism: Dunkels et al. [1] proposed a formula to calculate the energy consumption (E).

$$\frac{E}{V} = I_a t_a + I_l t_l + I_t t_t + I_r t_r + \sum I_c t_c \tag{4}$$

where V is the supply voltage, I_a and t_a are the current draw of the MCU (Microprocessor Control Unit) and time when the MCU has been running in active mode; I_l and t_l are the current draw and time of the MCU in low power or sleep mode; I_t and t_t are the current draw and the time of the communication device in transmit mode; I_r and t_r are the current draw and time of the communication device in receive mode; I_c and t_c are the current draw and time of other components such as sensors and LEDs. Then, the node current consumption (I) rate is equal to $\frac{E}{V \cdot t}$ where t is the time period. In this model, all current draw, supply voltage and temperature are assumed as fixed values (e.g., $3\,\mathrm{V}$ and $25\,^{\circ}\mathrm{C}$ as defined in the data sheet).

3) Temperature and Supply Voltage Effect: The current consumption of electronic circuit is affected by both temperature and supply voltage [2]. As temperature increases, current draw is increased. Liao et al. [29] proposed a leakage current model with temperature as:

$$I(T) = I_s \cdot \exp\left(\frac{-\alpha}{T - \beta}\right) \tag{5}$$

where T is the temperature in Kelvin, I_s is a constant current value, α and β are the empirical constants which are decided by the circuit designs. Later, supply voltage is considered for leakage calculation as [26]:

$$I(T, V_{dd}) = I_s(T_0, V_0) \cdot T^2 \cdot \exp\left(\frac{\alpha \cdot V_{dd} + \beta}{T}\right) \tag{6}$$

where T is the temperature in Kelvin, V_{dd} is the supply voltage, I_s is a constant current at the reference temperature T_0 and supply voltage V_0, α and β are the empirical constants which are decided by the circuit designs. It is assumed that the constant current (I_s) is already known.

C. Lifetime Estimation

The review of some lifetime estimation techniques for real world WSNs is presented as follows:

1) Based on Voltage Drop Rate: Hao et al. [30] proposed a technique for lifetime estimation as:

$$Lt = \frac{V_{init} - V_{cut}}{V_{rate}} \tag{7}$$

where V_{init} is the initial voltage of battery, V_{cut} is the cut-off voltage and V_{rate} is the voltage drop rate. In their experiments, it is observed that the average voltage drop rates are $16.5\,\mathrm{mV/day}$ for Mica2 and $21.5\,\mathrm{mV/day}$ for MicaZ. With an initial voltage level of $3.2\,\mathrm{V}$ and the cut-off voltage of $2.2\,\mathrm{V}$, the estimated lifetime are $60.6\,\mathrm{d}$ for a Mica2 and $46.5\,\mathrm{d}$ for a MicaZ.

2) Based on Quoted Capacity and Current Consumption: Selvig [31] presented a method to estimate the lifetime for sensor nodes based on CC2430 [32] as:

$$Lt = \frac{C}{\overline{I}} \tag{8}$$

where C is the battery capacity in mA h and $\overline{I}$ is the average current consumption. In this experiment, the battery capacity is assumed to be the quoted capacity from vendor and the average current consumption is measured by an oscilloscope. Since I=$\frac{E}{V \cdot t}$, the software-based technique can be applied for finding the average current consumption by using (4).

3) Based on Quoted Capacity and Energy Consumption: Landsiedel and Wehrle [33], proposed an energy monitoring model, called AEON, for a sensor node as:

$$E_{rem} = E_{current} - E \tag{9}$$

where $E_{current}$ is the current battery capacity in J, E_{rem} is the remaining battery capacity in J and E is the energy consumption which can be obtained by using (4). The initial value of $E_{current}$ is the initial capacity of battery in J. The battery capacity is also assumed to be the quoted capacity from vendor. For example, a pair of alkaline batteries with $2500\,\mathrm{mA\,h}$ of quoted capacity has $27\,000\,\mathrm{J}$ of the initial capacity. The lifetime of a node ends if E_{rem} of that node is empty. This model is implemented on top of AVRORA [34], a highly scalable sensor node simulator.

D. Summary and Discussion

Many SoC estimation techniques have been explored. Electrochemical methods require highly specific chemical knowledge which makes it difficult for real hardware implementation. Measuring the specific gravity is the uncomplicated

way, but it is difficult to apply to sealed batteries [17], [35]. Voltage measurement is an easy and popular method. However, this measurement technique is not always an accurate indicator [17], [35]. Moreover, it is impossible to take into account every point of voltage in order to provide an accurate SoC indication system. The EMF method is more accurately implementable for many battery types. However, other factors, such as temperature and ageing, must be considered. Load testing is an accurate and reliable battery capacity estimation technique but the load test equipment is required. The temperature effect proposed by Sheridan et al. is a generic model which can be applied for many battery types but it is difficult to find detailed information from a vendor's specifications, such as the activation energy and gas of the battery. The model proposed by Park et al. covered the remaining capacity and the effect of temperature on battery capacity. However, they assumed the battery began with full capacity voltage, which might not apply for NiMH batteries because this battery type has a relatively high self-discharge rate on the first day after full charging.

Several mechanisms are used for finding the current draw of sensor nodes. Although a hardware-based mechanism can provide accurate results, it is of significantly high cost and complexity for large scale usage. Moreover, it is difficult to add to the existing hardware. In contrast, a software-based mechanism is easy to add to the existing system without additional per-unit cost. However, fixed voltage and current draw values are assumed for current consumption calculation using a software-based technique, which may not be accurate in real-world deployments as the current draw is usually dynamic, based on temperature and supply voltage. Temperature and supply-voltage-effect formulae focus only on the effects of the leakage current draw. They do not provide methods for finding the constant current draw.

A lifetime estimation model based on the voltage drop is suitable for a static load application. However, it is difficult to be applied in the real deployment since the load of each sensor is normally dynamic, which leads to dynamic voltage drop. Moreover, this technique is not always an accurate indicator [17], [35]. The other two methods are widely used by many studies. However, thery are based on quoted capacity and do not take other impact factors on lifetime, such as temperature and consumption rate, into account.

As a result of accurate node lifetime estimation, the challenge is to propose a new generic technique for finding the battery capacity which covers temperature, ageing and self-discharging as well as other impact factors. Moreover, the software-based technique for finding the current consumption should be extended to cover the effect of temperature.

III. The Impact Factors on Lifetime

Here we analyse the many factors causing the different lifetime periods, such as battery types, models, brands, self-discharge, discharge rate, ageing, charge cycles and temperature.

A. Battery Types, Brands and Models

Table IV [12]–[14] shows the quoted capacity of two AA-size battery types: alkaline and NiMH, from several brands and models.

TABLE IV
Quoted Capacity for 100 mA Discharge to 0.9 V Cut-off at Room Temperature

Brands	Types	Models	Quoted Capacity (mA h)
A	Alkaline(AA-LR6)	A-Alkaline	2750
B	Alkaline(AA-LR6)	B-Alkaline	2750
C	Alkaline(AA-LR6)	C-Alkaline	2750
B	NiMH(AA-HR6)	B-NiMH1300	1430
B	NiMH(AA-HR6)	B-NiMH2000	2200
D	NiMH(AA-HR6)	D-NiMH2100	2310
D	NiMH(AA-HR6)	D-NiMH2500	2750

Based on the vendor data sheet, an AA-LR6 alkaline battery capacity for discharging at 100 mA to 0.9 V cut-off is around 2750 mA h [13], [14], while NiMH battery capacity is around 110% of the battery models, e.g., D-NiMH2100 model has 2310 mA h of quoted capacity. However, only 90% from quoted capacity can be used for discharging to a cut-off voltage of 1 V for alkaline batteries, while 93% can be used for NiMH batteries [12]–[14]. From (1), lifetime can be easily estimated by dividing that battery capacity with the current load and assuming k = 1. A constant 100 mA load generated by the CBA-III load tester is used for testing a pair of AA batteries at room temperature (22 °C). For NiMH batteries, they are charged by 500 mA charger and they are tested after being fully charged. The tested batteries are discharged until their terminal voltages reach the cut-off voltage at 2.0 V (of 2 cells). Table V shows the real measurement and estimation of lifetime. It is obvious that the battery model with high capacity has longer lifetime than the model with low capacity. With the same model of alkaline batteries, lifetime values of different brands have a little difference (±16 min). The differences between estimated lifetime based on vendor data sheet and real measurement lifetime are around 7 to 15%. These differences may be caused by other factors, such as self-discharging, ageing and charge cycles which will be described in the following subsection.

TABLE V
Measured and Estimated Lifetime of 100 mA Discharge to 2.0 V Cut-off at Room Temperature

Batteries	Lt (min)		Deviation
	Measured	Estimated	(%)
A-Alkaline	1384	1485	7.3
B-Alkaline	1370	1485	8.4
C-Alkaline	1368	1485	8.6
B-NiMH1300	694	796	14.8
B-NiMH2000	1144	1224	7.3
D-NiMH2100	1115	1285	11.5
D-NiMH2500	1410	1530	8.8

B. Self-discharge

Since alkaline batteries will lose approximately 2% of their capacity per year when stored at 20 °C due to the self-discharging process [13], [14], there is no significant effect on capacity for several months for this type of battery. This means that the starting voltage of alkaline batteries can be assumed to be 1.5V for each cell. In contrast, NiMH batteries have significantly high self-discharge of 20% on the first day and 1-4% per subsequent day. With self-discharging, they lose capacity and their voltages also drop. To study the relationship between starting terminal voltage (Vt) and lifetime, a CBA-III load tester with static 100 mA load testing runs with a pair of AA NiMH batteries from two brands, B-NiMH2000 and D-NiMH2500, on two different starting Vt at room temperature (22 °C). Lifetime periods from the starting Vt to the minimum Vt (cut-off at 2.0 V) are shown in Table VI.

TABLE VI
LIFETIME OF 100 mA LOAD WITH TWO AA NIMH BATTERIES

Battery	Starting Vt (V)	Measured Lt (min)
B-NiMH2000	2.81	1111
	2.88	1144
D-NiMH2500	2.71	1197
	2.85	1264

From this experiment, it is obvious that high starting Vt gives more lifetime period than low starting Vt. Higher starting Vt means the higher battery energy which results longer lifetime. The proposed lifetime equation for any starting Vt is:

$$Lt(Vt) = \left(-\tau \cdot \ln\left(\frac{Vt_r}{Vt}\right)\right) + Lt(Vt_r) \tag{10}$$

where τ is the time constant representing capacity affected by self-discharging and $Lt(Vt_r)$ is the lifetime of the reference voltage (Vt_r). The time constant τ can be obtained by the following equation [11].

$$\tau = \frac{t}{\ln\left(\frac{Vt_{r1}}{Vt_{r2}}\right)} \tag{11}$$

where t is the different time period between starting at Vt_{r1} and Vt_{r2} which is $Lt(Vt_{r1}) - Lt(Vt_{r2})$. From Table VI, t of B-NiMH2000 is -33 min, while t of D-NiMH2500 is -67 min. Vt_{r1} and Vt_{r2} of B-NiMH2000 are 2.81 V and 2.88 V, while they are 2.71 and 2.85 V for D-NiMH2500. Therefore, τ, Vt_r and $Lt(Vt_r)$ for B-NiMH2000 are 1341, 2.81, and 1111, while they are 1330, 2.71 and 1197 for D-NiMH2500. These values are then used for calculating lifetime (in minutes) with any Vt between Vt_{r1} and Vt_{r2} based on (10). Measured and estimated lifetime of B-NiMH2000 and D-NiMH2500 batteries with different starting voltages are shown in Table VII and VIII. The different starting voltages are caused by the self-discharging periods after full charging (1 h, 2 h, 3 h, 4 h and 5 h).

TABLE VII
MEASURED AND ESTIMATED LIFETIME FOR DIFFERENT STARTING VOLTAGE OF B-NIMH2000 BATTERIES

Voltage	Self-discharge	Lt (min)		Deviation
(V)	time (h)	Measured	Estimated	(%)
2.86	1	1138	1134	-0.3
2.85	2	1133	1130	-0.3
2.84	3	1127	1125	-0.2
2.84	4	1121	1125	0.4
2.83	5	1117	1121	0.3

TABLE VIII
MEASURED AND ESTIMATED LIFETIME FOR DIFFERENT STARTING VOLTAGE OF D-NIMH2500 BATTERIES

Voltage	Self-discharge	Lt (min)		Deviation
(V)	time (h)	Measured	Estimated	(%)
2.79	1	1250	1236	-1.1
2.78	2	1242	1231	-0.9
2.77	3	1235	1226	-0.7
2.76	4	1225	1221	-0.3
2.76	5	1223	1221	-0.1

C. Discharge Rate

The capacity of the battery varies with the rate of discharge. From the vendor data sheet with the discharge rate of 25 mA to 100 mA [13], [14], the capacity of the battery increases when the discharge rate decreases for alkaline batteries, while it decreases when the discharge rate decreases for NiMH batteries. If C in (1) is the capacity of batteries when they are discharged at 100 mA, peukert constant (k) values are 0.96 and 1.004 for alkaline AA-LR6 and NiMH batteries, respectively [13], [14]. These k constants are for a discharge rate of less than 100 mA. For example, if lifetime for a 100 mA discharge rate for alkaline batteries is 25 h (2500 mA h capacity), the lifetime for a 25 mA discharge rate will be 114 h (calculated from $\frac{2500}{25^{0.96}}$); and if a lifetime for a 100 mA discharge rate for NiMH batteries is 27.5 h (2750 mA h capacity), lifetime for 25 mA of discharge rate will be 108.5 h (calculated from $\frac{2750}{25^{1.004}}$).

D. Ageing

The capacity of batteries will vary depending on their ageing. Normally, battery packages have a date code on them indicating the use by date that the batteries can be used with good capacity (70-80% of quoted capacity) [11], [13]. Therefore, the ageing effect on lifetime is presented as:

$$Lt(a) = (1 - \rho \cdot a) \cdot Lt(new) \tag{12}$$

where a is the age of the battery in years, ρ is the ageing factor and $Lt(new)$ is the lifetime of the new battery. For examples, the capacity of alkaline batteries will reduce 2% per year [13], [14] when stored at room temperature (20 °C). This means that the lifetime of the device will be reduced 2% (ρ = 0.02) each year due to the age of the batteries. Therefore, the new AA-LR6 batteries will give 1350 min of lifetime for a device with 100 mA load, while they will give 1323 min of lifetime when storing these batteries for one year before using. For NiMH

batteries, the capacity will drop 6% (ρ = 0.06) per year due to their ageing when stored at room temperature [12], [13]. Therefore, the new D-NiMH2500 battery will give 1410 min after being fully charged, while they will give 1325 min after being fully charged if they have one year of age.

E. Charge Cycles

The charge cycles factor has an effect on rechargeable batteries by measuring how many times the batteries have been recharged. NiMH batteries can deliver 100% capacity for up to 300 charge cycles, while their capacity will reduce 0.1% for each charge cycle for more than 300 cycles [12], [13]. As a result, a decrease of lifetime can be described as:

$$Lt(c) = \begin{cases} Lt(new) & \text{if } c \leq 300 \\ (1.3 - 0.001c) \cdot Lt(new) & \text{otherwise} \end{cases} \quad (13)$$

where c is the number of charge cycles and $Lt(new)$ is the lifetime of the new battery. For example, the new D-NiMH2500 battery will give 1410 min, while they will give 1269 min at 400 charge cycles (c = 400).

F. Temperature

Both battery capacity and current consumption are affected by temperature. As temperature increases, the current draw is increased and, consequently, shortens the lifetime of the device. However for alkaline and NiMH cells, high temperature can provide increased capacity of battery over the operating temperature range 0 to 40 °C. Therefore, it depends on the ratio between increased battery capacity and current draw, which may result in increased or decreased lifetime. Based on (3) and information contained in vendor data sheets [12]–[14], [23], the constant A which depends on the activation energy and gas of the battery can be calculated as Table IX.

TABLE IX
CAPACITY OF DIFFERENT TEMPERATURES AND CONSTANT VALUE FOR DIFFERENT BATTERIES

Batteries	Capacity (mA h@0 °C)	Capacity (mA h@25 °C)	A
A-Alkaline	900	1950	2518.73
B-Alkaline	857	1942	2665.53
B-NiMH2000	1717	2113	677.19
D-NiMH2500	2127	2667	737.11

Based on (6), the leakage current draw at two different average temperatures in Kelvin (T_1, T_2) can be defined as:

$$\frac{I(T_2)}{I(T_1)} = \frac{T_2^2}{T_1^2} \cdot \exp\left(\frac{K \cdot (T_1 - T_2)}{T_1 \cdot T_2}\right) \quad (14)$$

where K is a constant depending on the circuit and V_{dd}. It is assumed that V_{dd} is the same for these two different temperatures. The real experiments have been conducted for Mica2 and N740 Nanosensor with a simple static load program at two different temperatures. The V_{dd} is static at 3.0 V. Table X shows the measured current draw by an ammeter and calculated K constant results.

TABLE X
CURRENT DRAW AT DIFFERENT TEMPERATURES AND K VALUE FOR MICA2 AND N740 MOTES

Sensor	Current (mA@5 °C)	Current (mA@25 °C)	K
Mica2	12	18	-1105.43
N740	47	66	-831.94

From (1), (3) and (14), node lifetime with full capacity at two different temperatures is derived as:

$$\frac{Lt(T_2)}{Lt(T_1)} = \frac{T_1^2}{T_2^2} \cdot \exp\left(\sigma \cdot \left(\frac{T_2 - T_1}{T_2 \cdot T_1}\right)\right) \quad (15)$$

where σ is the A + K values which can be obtained from Table IX and X and are presented in Table XI.

TABLE XI
RATIO CONSTANT VALUE OF DIFFERENT BATTERIES FOR MICA2 AND N740 MOTES

Sensor	Batteries	σ
Mica2	A-Alkaline	1413.30
Mica2	B-Alkaline	1560.10
Mica2	B-NiMH2000	-428.24
Mica2	D-NiMH2500	-368.33
N740	A-Alkaline	1686.80
N740	B-Alkaline	1833.59
N740	B-NiMH2000	-154.74
N740	D-NiMH2500	-94.83

The experiments are conducted to test the temperature effect on the lifetime of N740 mote with two NiMH batteries: B-NiMH2000 and D-NiMH2500. A simple program runs on different temperatures. This program load as measured by an ammeter at 25 °C is 67 mA. From Table IX, capacity of B-NiMH2000 and D-NiMH2500 batteries at 25 °C are 2113 and 2667 mA h. Therefore, node lifetime at 25 °C will be 31.01 h ($\frac{2113}{67^{1.004}}$) and 39.14 h ($\frac{2667}{67^{1.004}}$) for B-NiMH2000 and D-NiMH2500, respectively. However, the experiments run at temperatures between 19 to 24 °C. The results of real lifetime and estimated lifetime based on (15) including deviation are presented in Table XII.

TABLE XII
LIFETIME WITH DIFFERENT NIMH BATTERIES AND TEMPERATURES FOR N740 MOTES

Batteries	Temperature	Lt (min)		Deviation
	(°C)	Measured	Estimated	(%)
B-NiMH2000	20.0	1953	1941	-0.61
B-NiMH2000	21.0	1920	1924	0.21
B-NiMH2000	24.0	1885	1875	-0.53
D-NiMH2500	19.5	2462	2451	-0.45
D-NiMH2500	20.0	2445	2441	-0.16
D-NiMH2500	22.0	2417	2403	-0.58

IV. DNLE DESIGN AND IMPLEMENTATION

This research proposes formulae and processes for dynamic node lifetime estimation which covers many factors causing

the different lifetime periods, such as battery type, model, brand, self-discharge, discharge rate, ageing and temperature. These formulae do not require detailed electrical and electrochemical knowledge. Moreover, some limitations, such as memory and arithmetic capabilities, have to be taken into account for real implementation on sensor nodes. DNLE is based on the following assumptions for both alkaline and NiMH batteries. First, batteries from the same pack have the same performance and behaviour. Second, storing temperature does not affect the capacity change since the batteries are always stored at room temperature. Third, for NiMH batteries, charging method does not affect the capacity change since the same charger is used in these experiments. Fourth, temperature during charging does not affect the capacity change since the batteries are always charged at room temperature. Last, batteries have suffered fewer than 300 charging cycles.

A. DNLE Design

The following steps are proposed for finding the lifetime of each node:

1) Step 1: Finding the real battery capacities:

a) Alkaline Batteries: It is sometimes difficult to determine the battery capacity reduction due to ageing since the manufacture date is not available. Moreover, some batteries may have lower capacity than quoted. It can be assumed that batteries sampled from the same manufactured batch can be representative of that batch. Each sample pair is tested by the load testing with static 100 mA load in order to find the real battery capacity with cut-off voltage equal to the minimum voltage of sensor motes. In these experiments, the cut-off voltage is 2.2 V. After that, the real battery capacity (in mA h) can be calculated by:

$$C = Lt \cdot 100 \tag{16}$$

where Lt is the lifetime of the batteries in hours. For example, if a pair of alkaline batteries gives 22.5 h of lifetime, the capacity value is 2250 mA h. Instead of using quoted capacity, a sample average will be assigned as the capacity for batteries from this batch. The temperature (T_t) when running load testing is recorded. If T_i is the temperature when a node starts running, the initial capacity with temperature effect can be calculated by using (3) with T_2 as T_i and T_1 as T_t. We refer to this value as $C(T_i)$.

b) NiMH Batteries: For NiMH batteries, each sample pair is tested after full charging in a similar way to the alkaline type. However, since NiMH batteries have significantly high self-discharge on the first day, each sample pair is retested again after letting it 24 h of self-discharge. With self-discharging, the starting voltage of batteries is different from being fully charged. The starting voltage of fully charged batteries is referred as Vt_f and the starting voltage of batteries with 24 h of self-discharge is referred as Vt_{24h}. The capacities of two different starting voltages are referred as C_f for the capacity of fully charged batteries and C_{24h} for the capacity of 24 h of self-discharge batteries. Then, the battery capacity of any starting voltage (Vt) between Vt_{24h} and Vt_f can be calculated as:

$$C(Vt) = \left(-\tau \cdot \ln\left(\frac{Vt_{24h}}{Vt}\right)\right) + C(Vt_{24h}) \tag{17}$$

where τ is the constant representing capacity affected by self-discharging which can be obtained by:

$$\tau = \frac{c}{\ln\left(\frac{Vt_{24h}}{Vt_f}\right)} \tag{18}$$

where c is $C_{24h} - C_f$. It is assumed that the temperature (T_t) is the same when running load testing with fully charged and 24 h of self-discharge batteries. If T_i is the temperature when a node starts running, the initial capacity with temperature effect can be calculated by using (3) with T_2 as T_i and T_1 as T_t. We refer to this value as $C(Vt, T_i)$.

2) Step 2: Finding the current consumption every period: Adapted from (4) proposed by Dunkels et al., the current consumption at a period can be expressed as:

$$I = I_a t_a + I_l t_l + I_t t_t + I_r t_r + \sum I_c t_c \tag{19}$$

where I_a and t_a are the current consumption of the MCU (Microprocessor Control Unit) and the time when the MCU has been running in active mode during a period; I_l and t_l are the current consumption and time of the MCU in low power or sleep mode during a period; I_t and t_t are the current consumption and the time of the radio transceiver in transmit mode during a period; I_r and t_r are the current consumption and time of the radio transceiver in receive mode during a period; I_c and t_c are the current consumption and time of other components such as sensors and LEDs during a period. The calculation as this equation is applied based on device data sheet with temperature at 25 °C. The current consumption has to be calculated every period. Thus, the average current consumption ($\overline{I}$) for s periods can be computed by using the Simple Moving Average as:

$$\overline{I}(s) = \gamma \cdot \overline{I}(s-1) + (1-\gamma) \cdot I(s) \tag{20}$$

where γ is the weighting value = $\frac{s-1}{s}$, $\overline{I}(s-1)$ is average current consumption of the previous period, and $I(s)$ is the current consumption at the period s. If T is the temperature of the current period, the current consumption $I(s,T)$ and average current consumption $\overline{I}(s,T)$ can be calculated by using (14) with T_2 as T and T_1 as 298.15 (25 °C is 298.15 K).

3) Step 3: Remaining lifetime estimation: The remaining capacity (C_{rem}) at period s can be obtained by:

$$C_{rem}(s) = C_{rem}(s-1) - I(s,T)^k \tag{21}$$

where k is the peukert constant, $C_{rem}(s-1)$ is the remaining capacity before period s and it is equal to the initial capacity for the first period. This means that if s = 1, $C_{rem}(s-1)$ = $C(T_i)$ for alkaline batteries and $C_{rem}(s-1)$ = $C(Vt, T_i)$ for NiMH batteries. If T is the temperature of the current period, the temperature effect on the capacity is calculated by using (3), with T_2 as T and T_1 as the temperature of the previous period. We refer to this value as $C_{rem}(s,T)$. Finally,

the remaining lifetime at the current period and temperature Lt_{rem}(s,T) can be estimated as:

$$Lt_{rem}(s,T) = \frac{C_{rem}(s,T)}{\bar{I}(s,T)^k} \quad (22)$$

B. DNLE Implementation

DNLE has been implemented on two real hardware platforms, Mica2 and N740 NanoSensor with operating systems TinyOS and Contiki respectively. It was assumed that sensor motes support battery voltage and temperature reading. The process is as follows:

1) Process 1: Preconfigured and Starting process: Two AA-LR6 alkaline models (A-Alkaline and B-Alkaline) and two NiMH models (B-NiMH2000 and D-NiMH2500) are the batteries used in the experiments. The capacities of these battery packs are evaluated by using the CBA-III load tester with static 100 mA current at 25 °C. Three pairs of batteries are tested for finding the average values of each battery model. These average capacities are then used as the preconfigured values for sensor nodes. All preconfigured values are given in Table IX, X and XIII. All nodes may automatically obtain these preconfigured values during the discovery process, but it is out of scope in this research. When a node starts, it reads the current temperature and battery starting voltage in order to calculate the initial battery capacity as described in Step1 of the DNLE design section.

TABLE XIII
PRECONFIGURED CAPACITIES OF BATTERIES

Battery	Capacity at 25 °C (mA h)
A-Alkaline	1850
B-Alkaline	1800
B-NiMH2000	1585
D-NiMH2500	1814

2) Process 2: Looping process: We focus on three components: MCU, radio transceiver and sensing device, for finding the current consumption at runtime. The current draw of these components is configured based on the device data sheet. The device driver of these components is modified: time stamps are recorded when the components are turned on, and time differences are computed when the components are turned off. These time differences (with the same unit of the period) are used for the current consumption calculation based on (19). One minute is used as the time period (Step2 of the DNLE design section). Since the battery capacity is hours unit, it needs to be converted to the same unit of the period (e.g., 2000 mA h = 120 000 mA min for a period of 1 minute). Temperature readings are repeated every minute for updating the current temperature in order to calculate the effect on the current consumption, average current consumption, remaining capacity and remaining lifetime as described in Step2 and Step3 of the DNLE design section.

V. DNLE EVALUATION

This section evaluates the proposed technique on real testbed experiments with two different hardware platforms (Mica2 based on CC1000 radio and the ATMega128L [36], [37], and N740 Nanosensor based on CC2431 [32], [38], a SoC combining the CC2420 radio with 8051 MCU) and four battery models: A-Alkaline, B-Alkaline, B-NiMH2000 and D-NiMH2500. The N740 platform is implemented using Contiki OS, while Mica2 platform is implemented using TinyOS. Two techniques: Selvig's method and the DNLE are investigated. Lifetime estimation is made every minute. For Selvig's method, battery capacity is obtained by using quoted capacity as in Table IV, while the current consumption is calculated using (19). In these experiments 80 % of quoted capacity is used (as a cut-off voltage of 2.2 V) for alkaline batteries and 91 % for NiMH batteries [12]–[14]. Therefore, usable capacities are 2200 mA h for A-Alkaline, 2200 mA h for B-Alkaline, 2102 mA h for B-NiMH2000 and 2502 mA h for D-NiMH2500. For DNLE, the processes are as described in the DNLE design and implementation section. In general, the current consumption of the sensor node is less than 100 mA. Therefore, the peukert constant values are 0.96 and 1.004 for the alkaline and NiMH batteries, respectively.

These experiments consist of two nodes, the sender and the base station. The base station is placed in the normal room conditions, while the sender is placed in a controlled environment in order to operate under a static temperature (10 °C and 22 °C) as in Fig. 1. Two scenarios: static and dynamic loads are applied in the experiments.

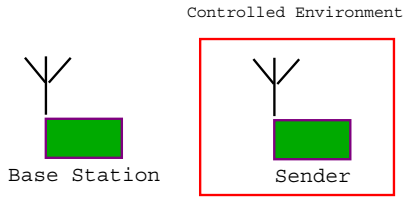

Fig. 1. Dynamic Node Lifetime Estimation Experiment

A. Scenario1: Static Load

For static load, the sender sends a fixed sized packet of 50 B to the base station every 3 s. Two sensor motes (Node1 and Node2) are used. Node1 runs as the sender for the first 3 times, while Node2 is the sender for the other 3 times. Lifetime estimation is calculated only at the sender node. NiMH batteries are given random starting voltages by a random self-discharging period of 5 min to 600 min. The average deviation results for two mote platforms with different battery models are shown in Table XIV. Since Selvig's method does not take some impact factors (such as charging rate, self-discharging and temperature) into account, the estimated values are much different from the measured ones around 19.1 % to 60.3 %. On the other hand, they are in the range of −3.5 % to 2.4 % for DNLE.

B. Scenario2: Dynamic Load

In a real deployment, a load of each sensor is normally dynamic, which may be caused by monitoring events or

TABLE XIV
AVERAGE DEVIATION OF STATIC LOAD LIFETIME ESTIMATION TESTBED RESULTS FOR MICA2 AND N740 MOTES WITH DIFFERENT BATTERIES

Sensor	Battery	Temp.	Estimated Lt Deviation(%)	
		(°C)	Selvig's Method	DNLE
Mica2	A-Alkaline	22	22.4	-1.0
Mica2	A-Alkaline	10	38.9	-1.4
Mica2	B-Alkaline	22	30.4	-2.5
Mica2	B-Alkaline	10	50.0	-3.5
Mica2	B-NiMH2000	22	60.3	1.5
Mica2	B-NiMH2000	10	33.3	2.4
Mica2	D-NiMH2500	22	53.4	-1.4
Mica2	D-NiMH2500	10	36.6	0.8
N740	A-Alkaline	22	19.1	1.7
N740	A-Alkaline	10	41.1	1.9
N740	B-Alkaline	22	26.3	-0.2
N740	B-Alkaline	10	50.9	-1.3
N740	B-NiMH2000	22	23.5	1.0
N740	B-NiMH2000	10	21.7	2.0
N740	D-NiMH2500	22	41.8	2.1
N740	D-NiMH2500	10	39.5	2.0

the number of neighbour nodes. For dynamic load in this experiment, the sender sends a packet of a random size of 20 B to 50 B to the base station every x seconds. The interval time value (x) was changed randomly every 10 min to between 3 s and 6 s. The testbed experiments run at temperatures of 10 and 22 °C. Two sensor motes (Node1 and Node2) are used. Node1 runs as the sender for the first 3 times, while Node2 is the sender for the other 3 times. Lifetime estimation is calculated only at the sender node. For NiMH batteries, they have random starting voltages by a random self-discharging period between 5 min to 600 min. The average deviation results for two mote platforms with different battery models are shown in Table XV. The deviation of Selvig's method is 18.7 % to 57.5 %, while it is −2.1 % to 2.5 % for DNLE.

TABLE XV
AVERAGE DEVIATION OF DYNAMIC LODE LIFETIME ESTIMATION TESTBED RESULTS FOR MICA2 AND N740 MOTES WITH DIFFERENT BATTERIES

Sensor	Battery	Temp.	Estimated Lt Deviation(%)	
		(°C)	Selvig's Method	DNLE
Mica2	A-Alkaline	22	21.0	-1.4
Mica2	A-Alkaline	10	37.8	-1.4
Mica2	B-Alkaline	22	30.6	-1.6
Mica2	B-Alkaline	10	57.5	2.1
Mica2	B-NiMH2000	22	33.9	2.5
Mica2	B-NiMH2000	10	22.4	-1.8
Mica2	D-NiMH2500	22	54.7	-0.6
Mica2	D-NiMH2500	10	32.8	-2.1
N740	A-Alkaline	22	18.7	1.4
N740	A-Alkaline	10	40.5	1.4
N740	B-Alkaline	22	26.0	-0.5
N740	B-Alkaline	10	50.2	-1.7
N740	B-NiMH2000	22	33.6	0.7
N740	B-NiMH2000	10	21.2	1.6
N740	D-NiMH2500	22	41.4	1.8
N740	D-NiMH2500	10	35.9	1.5

VI. CONCLUSIONS AND FUTURE WORK

In this paper, impact factors on node lifetime, such as battery brand, type, model, self-discharge, charging rate, battery ageing, charge cycles, and temperature, are investigated and analysed. Lifetime equations for any starting voltage, ageing, charge cycles and temperatures are proposed to explain the effect of the impact factors. Moreover, a dynamic node lifetime estimation technique, called DNLE is proposed. The experiments have been conducted on real hardware and software platforms in WSNs with different battery models. Two scenarios, dynamic and static loads, are implemented to evaluate the deviation of DNLE comparing to Selvig's method. The estimated values of Selvig's method are much different from the measured ones (around 18 % to 60 %), while they are close to the measured ones for DNLE (−3.5 % to 2.5 %) due to taking some impact factors into account, such as charging rate, self-discharging and temperature. It can be concluded that node lifetime can be predicted more accurately using DNLE, which can be applied for both off-line and on-line lifetime estimation.

Future work will include battery recovery effects when nodes employ dynamic duty cycling. Furthermore, the higher than room temperature and the impact of humidity should be investigated. In addition, the network lifetime will be further benefited with the integration of DNLE into the network routing process.

REFERENCES

[1] A. Dunkels, F. Osterlind, N. Tsiftes, and Z. He, "Software-based on-line energy estimation for sensor nodes," in *Proceedings of the 4th Workshop on Embedded Networked Sensors*, 2007, pp. 28–32.

[2] H. A. Nguyen, A. Forster, D. Puccinelli, and S. Giordano, "Sensor node lifetime: An experimental study," in *IEEE International Conference on Pervasive Computing and Communications Workshops, PERCOM Workshops*, 2011, pp. 202–207.

[3] W. Rukpakavong, I. Phillips, and L. Guan, "Neighbour discovery for transmit power adjustment in IEEE 802.15.4 using RSSI," in *New Technologies, Mobility and Security (NTMS), 2011 4th IFIP International Conference on*, feb. 2011, pp. 1–4.

[4] W. Rukpakavong, I. Phillips, L. Guan, and G. Oikonomou, "RPL router discovery for supporting energy-efficient transmission in single-hop 6LoWPAN," in *Communications (ICC), 2012 IEEE International Conference on*, jun. 2012, pp. 5721–5725.

[5] W. Rukpakavong, I. Phillips, and L. Guan, "Lifetime estimation of sensor device with AA NiMH batteries," in *IPCSIT vol. 55, International Conference on Information Communication and Management (ICICM)*, oct. 2012, pp. 98–102.

[6] Mica2 Wireless Measurement System. [Online]. Available: http://bullseye.xbow.com:81/Products/Product_pdf_files/Wireless_pdf/MICA2_Datasheet.pdf

[7] S. Ltd. (2008) Sensinode Ltd. joins Texas Instruments low-power RF developer network, offers IPv6 wireless network solutions based on 6lowpan standard technology. [Online]. Available: http://embedded-computing.com/sensinode-based-6lowpan-standard-technology

[8] U. Berkeley. (2004) What is tinyos? [Online]. Available: http://www.tinyos.net

[9] A. Dunkels, B. Gronvall, and T. Voigt, "Contiki - a lightweight and flexible operating system for tiny networked sensors," in *Proceedings of the 29th Annual IEEE International Conference on Local Computer Networks*, ser. LCN '04. Washington, DC, USA: IEEE Computer Society, 2004, pp. 455–462.

[10] G. Oikonomou and I. Phillips, "Experiences from porting the Contiki operating system to a popular hardware platform," in *Proceeding of 2011 International Conference on Distributed Computing in Sensor Systems and Workshops (DCOSS)*, Barcelona, Spain, Jun. 2011.

[11] H. Bergveld, W. Kruijt, and P. Notten, *Battery Management Systems: Design by Modelling (Philips Research Book Series)*. Springer, 2002.

[12] GP Battery Datasheet. [Online]. Available: http://www.gpbatteries.com

[13] Energizer Battery Datasheet. [Online]. Available: http://www.energizer.com

[14] Duracell Battery Datasheet. [Online]. Available: http://www.duracell.com
[15] Q. Zhang, Q. Guo, S. Liu, R. A. Dougal, and R. E. White, "Resistive companion modeling of batteries in a virtual test bed," *Journal of Power Sources*, vol. 141, no. 2, pp. 359–368, 2005.
[16] G. S. Nagarajan and J. V. Zee, "Characterization of the performance of commercial NiMH batteries," *Journal of Power Sources*, vol. 70, no. 2, pp. 173–180, 1998.
[17] V. P. Henk, H. J. Bergveld, D. Danilov, P. P. Regtien, and P. H. Notten, *Battery Management Systems: Accurate State-of-Charge Indication for Battery-Powered Applications*. Springer, 2008.
[18] B. Heyer, "One meter battery tester," US Patent 2,225,051, May 1938.
[19] W. Guoliang, L. Rengui, Z. Chunbo, and C. Chan, "State of charge estimation for NiMH battery based on electromotive force method," in *Vehicle Power and Propulsion Conference, VPPC '08*, sept. 2008, pp. 1–5.
[20] Z. Inc. (2008) The ZTS MBT-MIL multi-battery tester (MBT-MIL). [Online]. Available: http://www.ztsinc.com/MBTMIL_OI.pdf
[21] Ansmann. Ansmann energy check LCD battery tester. [Online]. Available: http://www.farnell.com/datasheets/39714.pdf
[22] W. M. Radio. Computerized battery analyzer (CBA). [Online]. Available: http://www.westmountainradio.com/cba.php
[23] C. Sheridan, J. Petersen, and J. Rohwer, "On modifying the Arrhenius equation to compensate for temperature changes for reactions within biological systems," in *Water SA*, vol. 38, no. 1, jan. 2012.
[24] B. Pierozynski, "On the low temperature performance of Nickel-Metal Hydride (NiMH) batteries," *International Journal of Electrochemical Science*, vol. 6, pp. 860–866, 2011.
[25] C. Park, K. Lahiri, and A. Ranghunathan, "Battery discharge characteristics of wireless sensor nodes: An experimental analysis," in *The 2nd Annual IEEE Communications Society Conference on Sensor and Ad Hoc Communications and Networks (SECON05)*, CA, USA, 2005.
[26] W. Liao, L. He, and K. M. Lepak, "Temperature and supply voltage aware performance and power modeling at microarchitecture level," *IEEE transaction on computer-aided design of integrated circuits and systems*, vol. 24, no. 7, pp. 1042–1053, jul. 2005.
[27] N. H. E. Weste and K. Eshraghian, *The Principles of CMOS VLSI Design*. Reading, U.K: MA:Addison-Wesley, 1993.
[28] X. Jiang, P. Dutta, D. Culler, , and I. Stoica, "Micro power meter for energy monitoring of wireless sensor networks at scale," in *Proceedings of the 6th international conference on Information processing in sensor networks, IPSN 07*, Massachusetts, USA, 2007, p. 186195.
[29] W. Liao, F. Li, and L. He, "Microarchitecture level power and thermal simulation considering temperature dependent leakage model," in *Proceedings of the 2003 international symposium on Low power electronics and design*, ser. ISLPED '03. New York, NY, USA: ACM, 2003, pp. 211–216.
[30] S. Hao, M. C. Chan, B. Anand, and A. L. Ananda. Structure health monitoring at MRT construction sites using wireless sensor networks link measurement at Pasir Panjang station. [Online]. Available: http://www.cir.nus.edu.sg/mrt-proj-report.pdf
[31] B. Selvig, "Measuring power consumption with CC2430 & Z-Stack," Application Note AN053(Rev. 1.0).
[32] "A True System on Chip solution for 2.4 GHz IEEE 802.15.4 / ZigBee®," CC2430 Data Sheet (Rev. 2.1), May 2007.
[33] O. Landsiedel and K. Wehrle, "AEON: Accurate prediction of power consumption in sensor networks," in *Proceedings of The Second IEEE Workshop on Embedded Networked Sensors (EmNetS-II)*, 2004.
[34] B. L. Titzer, "AVRORA: Scalable sensor network simulation with precise timing," in *Proceeding of the 4TH International Conference on information processing in Sensor Networks (IPSN)*, 2005, pp. 477–482.
[35] B. University. How to measure State-of-Charge. [Online]. Available: http://batteryuniversity.com/learn/article/how_to_measure_state_of_charge
[36] (2011) ATmega128/ATmega128L: 8-bit Atmel microcontroller with 128K-Bytes in-system programmable flash. [Online]. Available: http://www.atmel.com/Images/2467S.pdf
[37] "CC1000 Single Chip Very Low Power RF Transceiver," CC1000 Data Sheet.
[38] "System on Chip for 2.4 GHz ZigBee® / IEEE 802.15.4 with Location Engine," CC2431 Data Sheet (Rev. 2.0.1), May 2007.

Wilawan Rukpakavong graduated BSc in Computer Science from Thammasat University, M.Sc. in Computer Science from Asian Institute of Technology, and MSc in Computer Network from the University of Derby. She has served as a Lecturer at Thammasat University, Thailand since 1991. Now she is a PhD student at the Department of Computer Science, Loughborough University. Her research interests include efficient energy and lifetime of wireless sensor networks.

Lin Guan is a Senior Lecturer in the Department of Computer Science at Loughborough University. She received her PhD from the University of Bradford, UK, after which she was also appointed as a Research Associate. She then held a project manager/software engineer position in Simulation Systems Ltd shortly, prior to moving to Loughborough as a Lecturer in 2006. Her research interests focus on performance modelling/evaluation of heterogeneous computer networks, QoS analysis and enhancements, mobile computing and wireless sensor networks. She has published over 70 journal and conference papers and she has been serving as guest co-editor for several international journals, such as those published by Elsevier and Springer. During her PhD, she was awarded the British Federation of Women Graduates Foundation Main Grant in 2004. She holds two CASE awards and one EngD on EPSRC/BAE funded projects. She recently received a prestigious award as Royal Society Industry Fellow and EPSRC KTA project.

Iain Phillips has been involved in computing research for over 20 years, with over 100 publications in this area. His main work has been in network architectures considering performance and algorithms for the Internet and Wireless Sensor Networks.

He graduated from Manchester University with a BSc in Computing and Information Systems and a PhD in Computer Science - Thesis title Workload Distribution on Massively Parallel Machines. After 7 years post-doctoral research at Loughborough in the High Speed Networks group in Electrical Engineering (Research Assistant/Research Fellow), he moved to Loughborough Computer Science as a Lecturer in 1999, Senior Lecturer in 2005 and Head of Department 2008-11. From 2009-11 he was Vice Chair of the Council of Professors and Heads of Computing (CPHC) and from 2012-14 Chair. He is a Chartered Fellow of the BCS and a member of the ACM.